Indian Journal of Chemical Technology
Vol. 31, July 2024, pp. 631-641
DOI: 10.56042/ijct.v31i4. 9102

# Curcumin and ZnO-NPs loaded xanthan gum and hydroxypropyl guar gum-based hydrogel film for food packaging

Ishita Parmar, Meenakshi Tanwar & Rajinder K. Gupta*

Department of Applied Chemistry, Delhi Technological University, Delhi-110042, India

*E-mail: rkg67ap@yahoo.com

*Received 26 February 2024; accepted 22 May 2024*

This study is focused on the synthesis of a hydrogel based film for food packaging applications. Xanthan gum (XG) and hydroxypropyl guar gum (HPGG) based hydrogel films have been synthesized using citric acid (CA) as crosslinker, loaded with zinc oxide (ZnO) nanoparticles (NPs) and curcumin (Cur). The structural characteristics of hydrogel films is analysed by FTIR and XRD. Thermal analysis is conducted using TGA and morphological examination is done using SEM. Rheological analysis is performed to determine the viscoelastic behaviour of the hydrogel films. Anti-microbial assay, anti-oxidant assay and SRB assay are conducted to analyse the anti-bacterial, scavenging and cytotoxicity activity of the hydrogel films. The film shows biodegradability under compost environment in 30 days. Fruit shelf-life enhancer capabilities are also assessed by using an edible coating of strawberry. The results so obtained showed that the synthesized XG-HPGG-CA-ZnO-Cur Film has potential application in edible food packaging.

**Keywords:** Curcumin, Citric acid, Hydroxypropyl guar gum, Xanthan gum, ZnO

## Introduction

Food packaging materials ensure that the quality of food is maintained throughout its shelf life. Hydrogel is a beneficial approach for food packaging systems, especially in managing moisture, which can be a barrier to the longevity of food[1]. The primary purpose is to extend the life span of processed food products and maintain freshness, instead of being subjected to intricate and lengthy storage methods[2]. Due to their affordability and ability to withstand water exposure, plastic polymers have become a convenient and cost-effective choice for packaging. However, plastic films are not fully recyclable or biodegradable, leading environmentalists to look for materials derived from renewable resources[3].

Researchers have developed ecologically friendly packaging options, such as biopolymers, as a promising replacement for non-biodegradable plastics in food packaging[4]. Research is being conducted to enhance the performance of polymers by investigating superabsorbent hydrogel that can absorb water and other water-compatible fluids up to 100% of their dry weight[5]. Given the health risks associated with synthetic polymers and the surge in plastic waste, active packaging materials made from natural antimicrobial ingredients are gaining interest. Proteins, polysaccharides, and lipids are some diverse food-grade polymers being investigated for this purpose. Bio-based antimicrobial packaging can prevent undesired changes in food quality and ecological waste while carrying nutrients. These biodegradable polymers can be used as films or applied in the form of coatings to the food[6].

Bio-derived polymeric hydrogels offer an effective alternative for addressing the challenge of plastic packaging disposal in the context of food applications. Plasticused in food packaging, tends to be non-biodegradable, which poses an imminent threat to the environment. For the development of environmentally friendly packaging materials, a variety of renewable biopolymers, such as proteins, lipids, and their composites generated from plant and animal sources, have been studied as substitutes for their non-biodegradable petrochemical-based counterparts. In this study, a hydrogel-based film containing natural biopolymers is prepared to be used as a food packaging material. It also covers changes to the film's properties induced by biodegradation.

Xanthan gum (XG) is a high molecular weight acidic biopolymer obtained from (*Xanthomonas campestris)* during aerobic fermentation using corn or sugar cane derivatives. Its primary function is to thicken food and cosmetics due to its 2:2:1 molar ratio of d-glucosyl, d-mannosyl, and d-glucuronyl acid

residues along with varying amounts of pyruvyl groups[7]. XG exhibits hydrocolloid nature, making it highly functional in difficult settings such as high shear stress, high salt and acidic conditions. XG can also be used in small amounts to achieve zero-order release kinetics[8].

Another biopolymer with significant characteristics in food packaging is guar gum (GG), which is also a high molecular weight polysaccharide, obtained from *Cyamopsis tetragonolobus* embryos of the Leguminosae family. GG is composed of a polysaccharide chain consisting of mannose as the linear backbone and has a side chain made up of a [2:1] ratio of mannose to galactose[9]. Hydroxypropyl guar gum (HPGG), a derivative of GG, is created by reacting GG with propylene oxide. HPGG produces highly viscous and biodegradable solutions. HPGG is considered a better option in food packaging applications due to its greater thermal stability and solubility in comparison to GG[10].

Combining two biopolymers to synthesize hydrogels, increases their stability and usefulness[11]. Cross-linkers can enhance the mechanical properties of biopolymers, making them suitable for food packaging. Chemical crosslinking is the most effective method, particularly for biopolymers. Various crosslinking agents, such as $Ca^{2+}$ ions, citric acid, glutaraldehyde and boric acid can be used[4]. Covalent bonds, hydrogen bonds, ionic interactions, hydrophobic and dipole-dipole interactions can all crosslink polymer chains, resulting in hydrogels with various shapes such as films, coatings and sheets[11]. XG and HPGG crosslinked with CA forms a film which is useful in the application of food preservation.

Further, zinc oxide (ZnO) nanoparticles (NPs) possess antioxidant activity and properties of food preservation. Along with ZnO NPs, curcumin (Cur) show antioxidant and antimicrobial properties. Both ZnO NPs and Cur can enhance the property of the XG-HPGG based film.

The aim of this research is to develop a novel hydrogel-based film of XG and HPGG cross-linked with CA and loaded with ZnO NPs and Cur for food packaging applications. Moreover, thermal analysis (TGA), structural characteristics (FTIR and XRD), morphology (SEM), rheological measurement (viscosity, amplitude and frequency sweep) mechanical strength, fruit preservation, anti-microbial activity, anti-oxidant activity and cytotoxicity assay were analysed for the hydrogel-based films.

## Experimental Section

### Materials

XG was purchased from local market, HPGG was procured from Hindustan pvt. Ltd. Bhiwadi, India, as a gifted sample, CA was purchased from CDH, New Delhi, Cur from SD fine chemical, Mumbai and ZnO NPs were purchased from sigma Aldrich, USA. Glycerol was purchased from Fisher chemicals, UK. Milli Q water was used for all the experimental work.

### Synthesis of XG-HPGG-CA-ZnO-Cur hydrogel-based film

The food grade XG and HPGG were used for fabricating packaging hydrogel-based films. XG and HPGG being hydrophilic polymers easily dissolve in water. The ratio of [Gums: CA] was taken to be [1:1.5]. The required amount of XG and HPGG are dissolved in distilled water at a fixed interval of time. CA as a cross-linker was added to the homogenous solution of XG and HPGG. Glycerol was added as plasticizer to the homogenized solution. A fixed and same composition of [ZnO: Cur] was added to the hydrogel preparation with constant stirring for 3 h. Afterwards, sonication was done to remove entrapped air, then poured into Petri dish and left for drying in the oven at 45°C for 24 h. Subsequently, hydrogel-based films were made and then used for further characterization analysis. A control film i.e., XG-HPGG-CA was synthesized by same method without ZnO NPs and Cur.

### Characterization of hydrogel-based film

The Perkin-Elmer model 2000 FT-IR was used to perform analysis of functional groups in XG, HPGG, XG-HPGG-CA film, and XG-HPGG-CA-ZnO-Cur film. The data was collected in the range of 4000-400 $cm^{-1}$ by taking 32 scans at 4 $cm^{-1}$ resolution. X-ray diffraction was conducted using a wide-angle X-ray diffractometer. Bruker D8 Advance was used with Cu-Kα radiations of λ = 1.5406 Å, a scanning range of 2θ (5°–80°), and a scan rate of 1°/min at 20 kV and a current of 10 mA. The SEM (JEOL JSM-6610LV) was utilized to examine the surface morphology of the samples at 500, 1000, and 2500X magnifications under an accelerating voltage of 20 kV. To determine the thermal stability of the samples, TGA (TGA 4000) was used. The samples were heated from 25°C to 800°C at a heating rate of 10°C/min in $N_2$ atmosphere. Using Anton Paar Modular Compact Rheometer 302 (MCR), the rheological properties of XG-HPGG-CA solution and XG-HPGG-CA-ZnO-Cur solutions were determined at room temperature. The tests were conducted using a 40 mm parallel plate.

The mechanical properties of XG-HPGG-CA-ZnO-Cur Film were analysed by a Universal Testing Machine (UTM), LLOYD LR 5K. Load range was 1-50 N with a 1000 mm extension range and 5 mm gauge length. The test and approach speed were 500 mm/min with no preload. A strip of 15 mm width and 150 mm length was cut from each film for mechanical testing. Under air conditions, three readings were taken for each sample and the average result was evaluated for mechanical properties of the film.

To evaluate the antimicrobial activity of the films, the agar disk diffusion method was used against *Escherichia coli* and *Staphylococcus aureus*, representing Gram-negative and Gram-positive bacterial strains respectively. Bacterial cultures were prepared in nutrient broth and inoculated onto agar plates. Disks were cut from each film and put on the plates. The fully formed zones (ffz) were measured using a digital calliper after incubating the plates for 14-16 h at 37°C. The films used in the experiment were 0.7 cm in diameter. In order to conduct a comparative study regarding the rate of food spoilage, fresh strawberries were taken. One strawberry was coated with synthesized hydrogel and the other was used in uncoated form and stored in glass petri plates. Samples were tested at regular intervals of 24 h for 1 week. All studies were conducted in natural lighting at a constant temperature of 25℃. The UV-visible spectrophotometer was used to evaluate the antioxidant activity of hydrogel solution by DPPH free-radical scavenging[12]. A modified method based on a previous study was used to determine the photochemical stability, in which varying amounts of hydrogel solution (3 mg, 5 mg, 7 mg, 20 mg, and 50 mg) of XG-HPGG-CA-ZnO-Cur solution were dissolved in 50 mL ethanol solution at 37°C[13]. Eq. (1) was used to determine the percentage of DPPH scavenging activity after mixing 1 mL of the solution with 3 mL of ethanol solution containing DPPH (1 mg/20 mL) and incubating it in the dark at room temperature for 30 min. The absorbance was measured at 517 nm.

$$\text{Scavenging activity of DPPH (\%)} = \left(1 - \frac{A_{sample}}{A_{control}}\right) x\ 100 \quad \ldots(1)$$

The value of $A_{control}$ indicates the absorbance of 1 mL ethanol and 3 mL ethanol solution of DPPH, while $A_{sample}$ refers to the absorbance of 1 mL XG-HPGG-CA-ZnO-Cur solution and 3 mL DPPH solution, as stated in prior research[14].

The degradation tests were performed on XG-HPGG-CA-ZnO-Cur Film by the method of burring the film in standard soil (ISO 17556 standard soil) for 30 days at room temperature and moisture-controlled conditions. The film was buried 2 cm under the soil. The buried film was removed from the soil, gently brushed and washed with distilled water, dried and analysed for weight loss after every 5 days. The weight loss was observed through TGA. As a fragment of film was studied for weight loss and compared it with the freshly prepared film. The percentage weight loss was calculated as by Eq. (2),

$$\text{Percentage weight loss} = \left(\frac{w_i - w_f}{wi_i}\right) \text{x } 100 \quad \ldots(2)$$

Where $w_i$ is the initial weight of the film and $w_f$ is the weight after 5 days interval.

The cytotoxicity of the films using Hep-G2 cell line was determined using the SRB assay[15]. In the initial stage, cells were cultured in a 96-well plate with DMEM medium supplemented with 10% FBS and 1% antibiotic solution, at a density of 8000 cells/well, and incubated at 37°C with 5% $CO_2$. Following 24 h, the cells were exposed to varying concentrations of the dose (ranging from 0.05-1.25%), prepared in an incomplete medium. After an additional 24 h of incubation, each well was treated with 100 µL of 10% trichloro acetic acid (TCA) and incubated for 1 h. The plate was then washed with DM water and allowed to air dry at room temperature, followed by the addition of a final concentration of 0.04% SRB solution to each well, and incubated for 1 h. Once incubation was complete, the plate was rinsed with 1% (v/v) acetic acid to eliminate any unbound dye and left to air-dry at room temperature. To solubilize the protein-bound dye, a Tris base solution (pH=10.5) was introduced to each well and agitated for 10 min using an orbital shaker. Finally, the plate was examined in an ELISA plate reader (iMark, Biorad, USA) at 510 nm.

## Results and Discussion

### FTIR

FTIR was carried out on XG, HPGG, XG-HPGG-CA film and XG-HPGG-CA-ZnO-Cur film to determine their functional groups in the range of 4000-400 $cm^{-1}$ as shown in Fig. 1. XG showed characteristic peaks at 3325 $cm^{-1}$ for O-H stretching and 1608 $cm^{-1}$ for C=C stretching vibrations[16]. HPGG showed characteristic peaks at 2912 $cm^{-1}$ for C-H stretching, 3342 $cm^{-1}$ for N-H stretching and

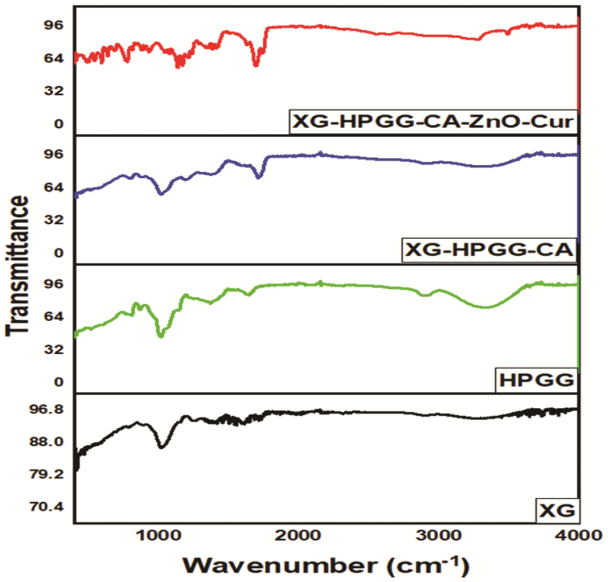


Fig. 1 — FTIR spectra of XG, HPGG, XG-HPGG-CA film and XG-HPGG-CA-ZnO-Cur film

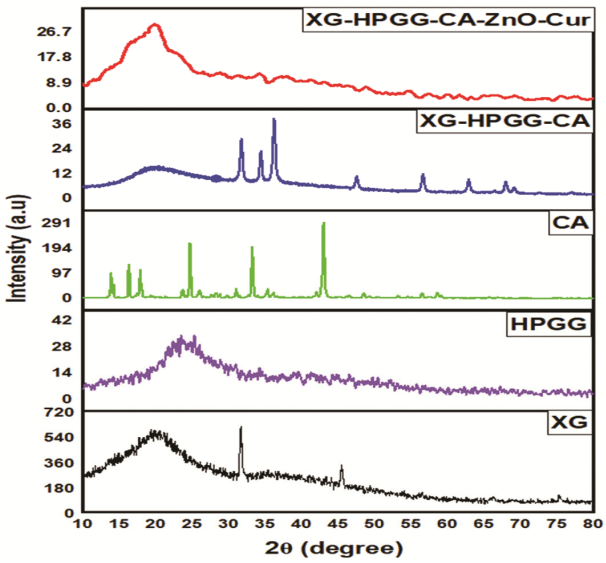


Fig. 2 — X-ray diffractogram of XG, HPGG, CA, XG-HPGG-CA film and XG-HPGG-CA-ZnO-Cur film

1635 $cm^{-1}$ for C=O stretching vibrations[17]. The FTIR spectra of XG-HPGG-CA showed a significant shift in peak from XG and HPGG at 3360 $cm^{-1}$, 2921 $cm^{-1}$ and 1722 $cm^{-1}$ due to crosslinking with CA. The FTIR spectra of XG-HPGG-CA-ZnO-Cur film showed a significant peak at 3273 $cm^{-1}$, corresponding to the -OH stretching vibrations, and 1697 $cm^{-1}$, due to carbonyl (C=O) stretching vibrations[18]. These shifts are majorly due to esterification with CA and incorporation of ZnO and Cur, which are essential in various applications, including food packaging[11].

**XRD**

The x-ray diffractogram of XG, HPGG, CA,XG-HPGG-CA film and XG-HPGG-CA-Cur-ZnO film are shown in Fig. 2. HPGG and XG exhibited broad peaks at 23.8° and 20.4°, respectively. CA showed peaks at 14º, 16º, 17º, 24.7º, 33º and 43º. XG-HPGG-CA film displayed a similar peak at 18.64° due to cross-linking of the two gums with CA. The shift of peaks was observed in XG-HPGG-CA-Cur-ZnO Film at 19.92º due to esterification. XRD patterns of XG, HPGG, XG-HPGG-CA film and XG-HPGG-CA-ZnO-Cur film showed amorphous structure with low overall crystallinity. The crystalline regions of XG and HPGG were due to hydroxyl groups at18.86°and 19.96°, respectively. The stability of XG and HPGG was maintained by hydrogen bonds, which when broken, led to a decrease of crystallinity in XG-HPGG-CA film and XG-HPGG-CA-ZnO-Cur film[19-22].

**SEM**

SEM images of XG-HPGG-CA film and XG-HPGG-CA-ZnO-Cur film are shown in Fig. 3 at 500X and 1000X magnifications. SEM has been demonstrated to be quite useful for determining and verifying morphological traits[23,24]. The interior structure of the film was heterogeneous and inter-linked, which can result in significant swelling and permeability as well as facilitate cellular growth. Crosslinking of XG and HPGG with CA was responsible for homogeneous covering of XG-HPGG-CA film in Fig. 3c. On adding ZnO and Cur to the XG-HPGG-CA film, the morphology of the film changed from smooth surfaces to rough and hollow-follicular, as shown in Fig. 3(a,b). This shift in morphology after cross linking is due to the presence of ZnO and Cur constituents and the irregular pore network structure in XG-HPGG-CA-ZnO-Cur film is responsible for the heterogeneity in the polymeric hydrogel[25]. These structural characteristics provide additional evidence that cross-linked hydrogel networks were formed during the polymerization phase[26]. The surface morphology of polymers can provide valuable information regarding their specific pore size distribution or specific areas of the polymer matrix[14]. The structure of XG-HPGG-CA-ZnO-Cur film, as revealed by the surface morphology shows that this biopolymer is well suited to be used as a food packaging material[27].

**TGA**

TGA of XG, HPGG, CA, XG-HPGG-CA film, and XG-HPGG-CA-ZnO-Cur film is shown in Fig. 4. In

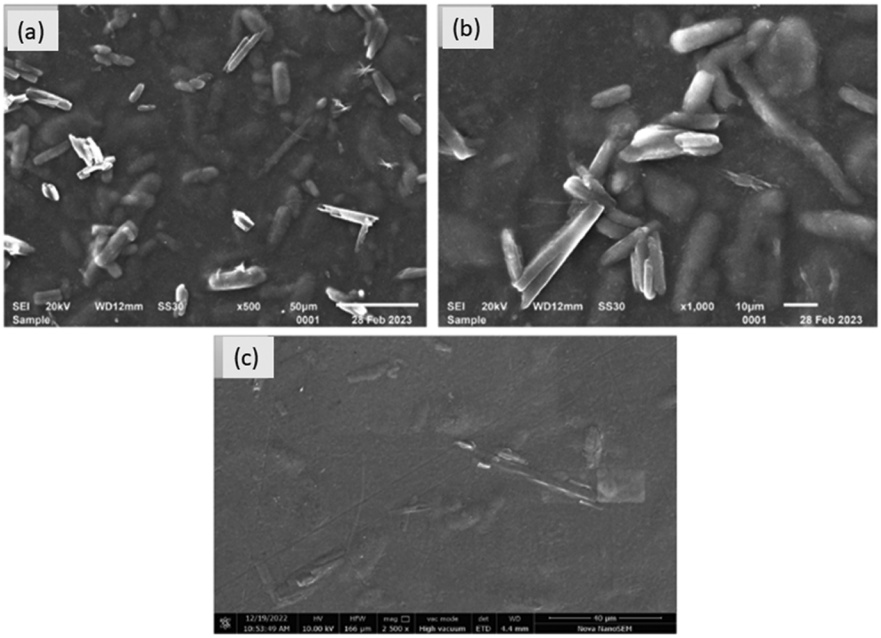


Fig. 3 — SEM micrographs at different magnifications of (a, b) XG-HPGG-CA-ZnO-Cur film at 500 and 1000X magnifications, respectively and (c) XG-HPGG-CA film at 2500X magnifications

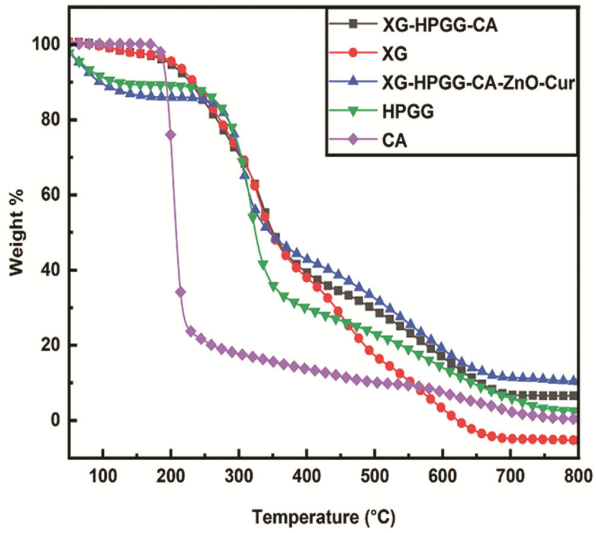


Fig. 4 — TGA of CA, HPGG, XG, XG-HPGG-CA film and XG-HPGG-CA-ZnO-Cur film

each instance, the initial decomposition temperature (IDT) was employed to adjust for any loss of weight. For XG, an IDT of 13.66% was observed at (29°C to 222.27°C), while HPGG showed an IDT of 8.94% at (45.26°C to 183.92°C). IDT for CA was observed to be 83.772% at (163.68°C to 332.63°C). The crosslinked polymers, XG-HPGG-CA film and XG-HPGG-CA-ZnO-Cur film, showed a weight loss of 3.239% and 2.268%, respectively, within almost the same temperature range. This demonstrates the added stability of XG-HPGG-CA-ZnO-Cur film was due to the presence of ZnO and Cur. $T_{max}$ is the temperature at which the maximum rate of weight loss occurs[1], was observed in the range of (222.27°C to 418.32°C), (183.92°C to 392.92°C), (17.089°C to 388.9°C), and (151.2°C to 461.7°C) for XG, HPGG, XG-HPGG-CA film, and XG-HPGG-CA-ZnO-Cur film, respectively. These observations indicate that the thermal stability of gums, such as XG and HPGG, decreases during the stages of decomposition, but the polymerization and formation of films of XG-HPGG-CA film and XG-HPGG-CA-ZnO-Cur film, showed an increased degree of stability due to the less percentage of weight loss compared to XG and HPGG[28].

**Viscosity**

Rheology is the scientific study of the deformation and flow of matter, which elucidates the relationship between force, time and deformation. It is the experimental method employed to assess the rheological characteristics of materials[29]. Shear rheological testing was conducted by varying the shear rate from 10 $s^{-1}$ to 100 $s^{-1}$. Throughout the shear rate range, it was observed that XG-HPGG-CA-ZnO-Cur solution exhibited a stronger shear thinning behaviour than XG-HPGG-CA solution as shown in Fig. 5a. The significant shear-thinning characteristics were attributed to the incorporation of ZnO and Cur in

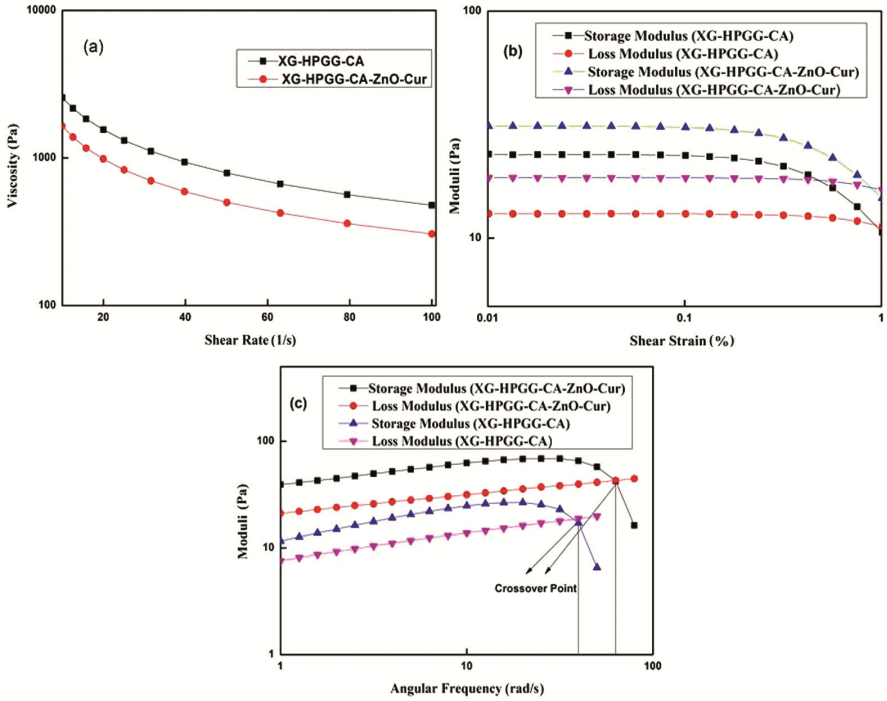


Fig. 5 — (a) Shear viscosity profile (b) amplitude sweep and (c) frequency sweep of XG-HPGG-CA solution and XG-HPGG-CA-ZnO-Cur solution

the XG-HPGG-CA-ZnO-Cur solution composition. In both cases, a considerable reduction in viscosity was observed due to the shear-induced alignment of XG-HPGG-CA solution and XG-HPGG-CA-ZnO-Cur solution in the flow direction[30].

**Amplitude sweep**

The amplitude sweep was conducted to determine the upper and lower limits of the linear viscoelastic (LVE) range and to assess the hydrogel's structural and mechanical stability[31]. Fig. 5b illustrates the plotted results of the storage modulus G' and loss modulus G" against shear strain percentage. The LVE range was characterized by a constant G' at low deformation, indicating that the sample structure remained intact[32]. At lower strain, both XG-HPGG-CA-ZnO-Cur solution and XG-HPGG-CA solution behaved as viscoelastic solids, while at higher strain, they behaved as viscoelastic fluids due to the disturbance of the structure, indicating the end of the LVE-region. The sample's rigidity at rest is characterized by the plateau value G′ within the LVE region. The LVE range for XG-HPGG-CA-ZnO-Cur solution was found to be G′=29.8 Pa, and for XG-HPGG-CA solution, G′=22.9 Pa, due to the addition of Cur and ZnO. When the sample reaches its most solid state, the LVR typically ends. The shear modulus at this point was observed to recover around 80% of its initial value[33]. The solution with ZnO and Cur showed a lower critical value (γc) of 18.6% compared to the solution with XG-HPGG-CA (γc) of 13%.

**Frequency sweep**

The frequency sweep test is used to assess the viscoelastic properties of a material by comparing the values of G' and G" over a range of frequencies[34]. Ajovalasit *et* al. conducted a study to investigate the effects on G' and G" within a frequency range by adding additives and concluded that all hydrogels showed the viscoelastic nature and found that both G' and G" showed positive slopes with the loss modulus increasing more rapidly compared to the storage modulus[35]. Throughout the test, the shear strain percentage was kept constant in the LVE region and frequency varied from 1 to 100 rad/s. The results in Fig. 5c show that for both XG-HPGG-CA solution and XG-HPGG-CA-ZnO-Cur solution solutions, G" dominates at high frequency while G' dominates at low frequency, indicating a viscoelastic solid behaviour and the Moduli of XG-HPGG-CA-ZnO-Cur solution is higher than XG-HPGG-CA hydrogel solution at all frequencies which proves extra stability due to ZnO and Cur.

Table 1 — Mechanical properties

| Film | Maximum force (N) | Tensile strength (MPa) | Elongation at break (%) |
|---|---|---|---|
| XG-HPGG-CA film | 49.5 ± 0.54 | 28.4 ± 0.10 | 8.9 ± 0.24 |
| XG-HPGG-CA-ZnO-Cur film | 54.6 ± 0.42 | 29.7 ± 0.15 | 7.88± 0.54 |

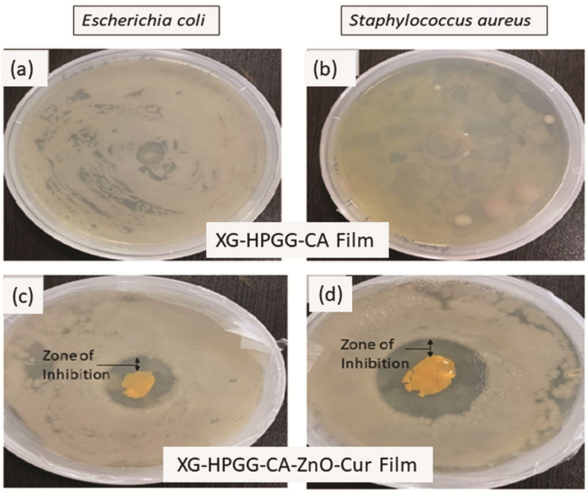


Fig. 6 — Disk diffusion test against *Escherichia coli* (a and c) and *Staphylococcus aureus* (b and d) for XG-HPGG-CA Film (a ,b) and XG-HPGG-CA-ZnO-Cur Film (c, d).

**Mechanical Properties**

The tensile properties of XG-HPGG-CA and XG-HPGG-CA-ZnO-Cur films were studied. The results for thickness (mm), width (mm), maximum load (N), elongation at break (%) and tensile strength (MPa) of the film are shown in the Table 1.

The XG-HPGG-CA-ZnO-Cur film showed an elongation at break % of 7.88 ± 0.54 which indicated its ability to withstand stretching and deformation before breaking. It has a high tensile strength of 29.7 ± 0.15 MPa which was indicative of its ability to withstand tension and resist breaking under force. These properties have made this film suitable for biomedical applications such as food packaging material.

***In Vitro* Test**

**Disk Diffusion test**

Active food packaging technology, involving incorporation of antimicrobial agents in the packaging to prevent microbial growth and prolong the shelf life of food, is becoming popular[36]. Fig. 6 shows the results of testing the antimicrobial activity of XG-HPGG-CA film and XG-HPGG-CA-ZnO-Cur film composites against two bacterial pathogen strains, *Escherichia coli* and *Staphylococcus aureus* using the disk diffusion method. In Fig. 6(a,b), XG-HPGG-CA film did not exhibit any antibacterial activity against either *E. coli* or *S. aureus* and it could not penetrate the bacterial cell. However, XG-HPGG-CA-ZnO-Cur film, (Fig. 6 (c, d) demonstrated a clear zone of inhibition of 87 mm and 102 mm, respectively, against both *E. coli*. and *S. aureus*. The results imply that XG-HPGG-CA-ZnO-Cur film exhibits significant antibacterial properties against both Gram-negative and Gram-positive bacteria, indicating that it has a broad-spectrum antibacterial activity.

The presence of an inhibition zone in the XG-HPGG-CA-ZnO-Cur film nanocomposite suggests that the biocidal action of ZnO NPs involves disrupting the membrane by generating surface oxygen species rapidly, ultimately leading to the death of pathogens[37]. This demonstrates the potential of XG-HPGG-CA-ZnO-Cur film composites as an effective active food packaging technology for inhibiting microbial growth and extending the shelf life of food products.

**Food sampling test**

After conducting antimicrobial tests using the disk diffusion method, the films were evaluated as a potential food packaging material for a food sample coated with hydrogel and a comparison was made with non-coated food material. To create a protective layer over the surface, the strawberries were directly immersed in the XG-HPGG-CA-ZnO-Cur solution and left to air dry[38]. Although strawberries have high antioxidant properties, their susceptibility to mechanical damage can lead to infectious symptoms, and their postharvest life is limited to about five days at 4°C[39]. The study aimed to enhance the shelf life of strawberries by coating them with an effective solution of prepared hydrogel.

Fig. 7 depicts one strawberry coated with the XG-HPGG-CA-ZnO-Cur solution while the other remains uncoated. The XG-HPGG-CA-ZnO-Cur solution coated strawberry showed slower deterioration compared to the uncoated sample. Day-1, showed no microbial growth on either of the fruit samples. Day 3, showed microbial growth on the non-coated fruit sample, and the fruit was shown to be deteriorated by Day 7. On the other hand, no microbial growth is observed on the strawberries coated with XG-HPGG-CA-ZnO-Cur solution coating till day 7. All these results confirm XG-HPGG-ZnO-Cur solution as a potential food packaging material with antimicrobial characteristics and Cur and ZnO as effective ingredients in active packaging films. Fruits and

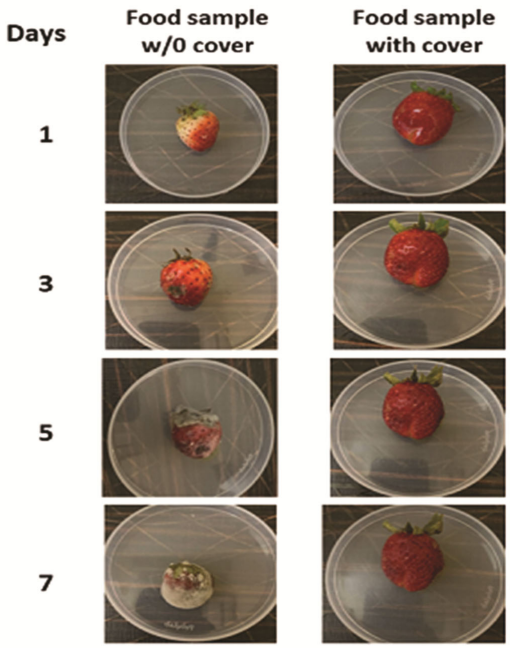


Fig. 7 — Food sample testing using strawberry without coating and with coating of XG-HPGG-CA-ZnO-Cur solution

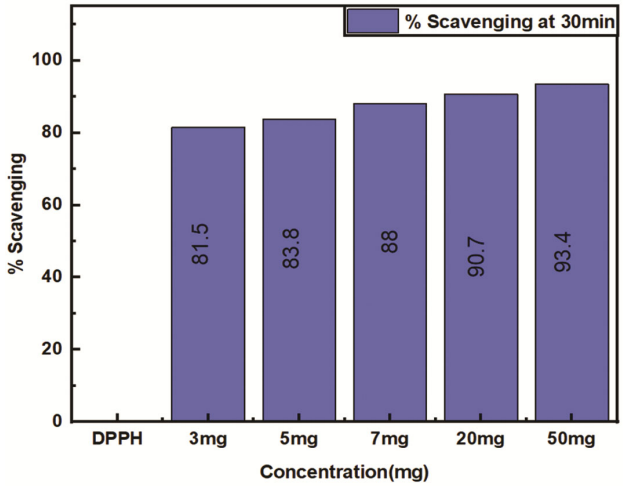


Fig. 8 — Scavenging of $DPPH^+$ radical by XG-HPGG-CA-ZnO-Cur film

vegetables with a high respiration rate can also be packaged using biopolymer sheets with a water permeability function[40].

**Antioxidant activity**

Although the conjugated diene moiety found in Cur accounts for the majority of its activities, the nearby phenolic groups have also been implicated in its antioxidant properties in Fig. 8. The results of the $DPPH^+$ Assay demonstrated that Cur facilitated hydrogen atom transfer, leading to conversion of a

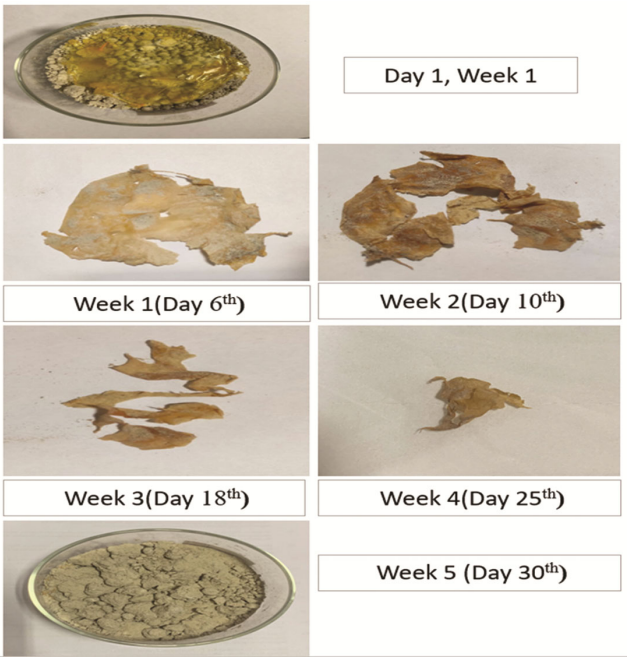


Figure. 9 — Biodegradation of XG-HPGG-CA-ZnO-Cur film

Table 2 — Biodegradability assay: XG-HPGG-CA-ZnO-Cur film weight loss

| Day | Initial weight (g) | Final weight (g) | Percentage weight loss |
|---|---|---|---|
| 5 | 0.472 | 0.337 | 28.6% |
| 10 | 0.315 | 0.194 | 38.4% |
| 15 | 0.194 | 0.093 | 52% |
| 20 | 0.093 | 0.039 | 58% |
| 25 | 0.039 | 0.085 | 78.2% |
| 30 | 0.085 | 0.000 | 100% |

stable radical called 2,2-diphenyl-1-picryl hydrazyl into 2,2-dipheny-l-picryl hydrazine (diamagnetic, non-radical)[41]. The assay showed a trend of increasing antioxidant activity. The combination of ZnO nanoparticles and Cur exhibited significant antioxidant activity against $DPPH^+$ free radicals[42]. The antioxidant activity was evaluated by incubating the solutions of varying concentrations (3 mg, 5 mg, 7 mg, 20 mg, 50 mg) with $DPPH^+$ solution for 30 min, resulting in an increase in antioxidant activity of 81.5%, 83.8%, 88%, 90.7% and 93.4%, respectively. The antioxidant activity of food packaging film can positively impact the packaging process by regulating the production of reactive oxygen species[43].

**Biodegradability test using soil burial method**

The results of the biodegradability test using soil burial method have been shown in the Fig. 9 and degradation was calculated at the interval of every 5 days that was shown in Table 2. It has been

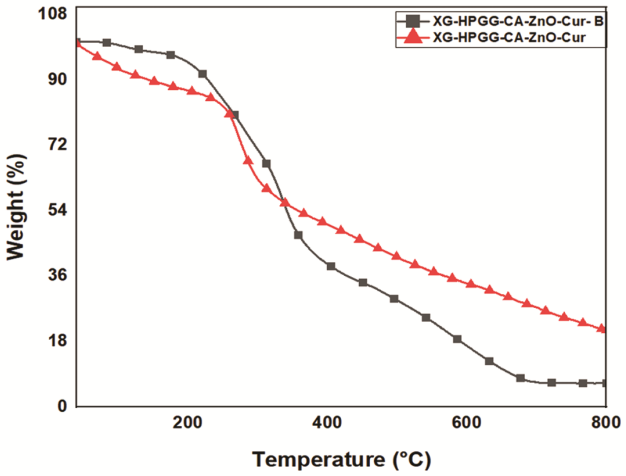


Fig. 10 — TGA graph of initial XG-HPGG-CA-ZnO-Cur film and the same film upon biodegradation (XG-HPGG-CA-ZnO-Cur –B)

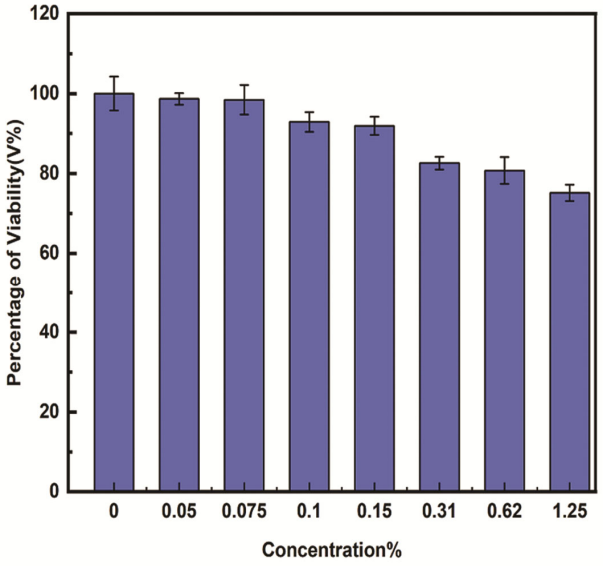


Fig. 11 — The viability percentage of Hep-G2 cells, for XG-HPGG-CA-ZnO-Cur film

observed that longer the burial time, higher will be the degradation of the film, which proved the environmentally friendly properties of the film[44]. The film gradually started to break down into small fragments around day-6 of first week after burial. Deterioration of film was seen on the surface as the film became fragile further in week 2. Cracks were observed on the surface of the sample all along the coming weeks of week 3 and week 4 as the film broke down in further smaller fragments. Soil degradation influenced macrostructural changes. Most of the film was degraded by the end of week 4 and only a small section of the film could be seen. The film was seen to be completely degraded around day 30$^{th}$ in week 5.

The film was weighed to calculate the weight loss over the period of degradation of 5 days. On around 5$^{th}$ day in week 1, the film was dusted and washed with distilled water to perform thermal degradation analysis. The results were then compared with an initial bioactive film as shown in Fig. 10. Shifts in peaks of both the films and amount of residual content was observed which further led to the observation that components of the biodegraded film broke down due to natural decomposition of the film upon microbial action in the soil. The biodegraded film showed wt. loss at a much faster rate than the XG-HPGG-CA-ZnO-Cur Film. Hence, it could be concluded that XG-HPGG-CA-ZnO-Cur Film is biodegradable film, which is an important aspect in packaging applications.

**Cytotoxicity evaluation by SRB Essay**

The cytocompatibility of XG-HPGG-CA-ZnO-Cur films was assessed using human hepatic cell lines (Hep-G2) as model cell lines. The results of the cytotoxicity test for different concentrations are presented in Fig. 11. The experiment with Hep-G2 cell culture demonstrated that the cells were able to attach to the surfaces of the films, proliferate, and disseminate[15]. After the incubation period, the cells on the XG-HPGG-CA-ZnO-Cur films exhibited normal morphology. The viability values of all film samples at different concentrations as shown in Fig. 11 were above 80%, indicating that the films were biocompatible with Hep-G2 cells.

## Conclusion

This study demonstrated the successful fabrication of XG-HPGG-CA-ZnO-Cur films with antimicrobial properties and a strong zone of inhibition, making them suitable for use as edible food packaging material. The addition of glycerol also improved their thermal and mechanical stability compared to XG-HPGG-CA-ZnO-Cur. The characterization of the samples using various analytical techniques, such as FTIR, XRD, SEM, TGA, rheology, *in-vitro* tests revealed that XG-HPGG-CA-ZnO-Cur films promoted cell growth and differentiation, indicating their potential as a food packaging material. The films have antimicrobial, antioxidant properties and show biodegradable properties. These findings suggest that the use of harmful plastics in food packaging could potentially be reduced by utilizing these edible and affordable options. Overall, XG-HPGG-CA-ZnO-Cur films show promise as a sustainable and biocompatible alternative for food packaging applications.

## Acknowledgements

The authors would like to thank Dr. Swarmita Dixit (Aakaar Biotechnologies Pvt. Ltd., Jankipuram Extension, Lucknow, India) for carrying out SRB test for the synthesized XG-HPGG-CA-ZnO-Cur Film. The authors are also thankful to UFlex Pvt. Ltd. Noida, India, for mechanical strength testing. Furthermore, the authors acknowledge the Vice Chancellor of DTU, for supporting the project with research facilities and financial aid.

## References

1 Kang M, Oderinde O, Liu S, Huang Q, Ma W, Yao F & Fu G, Characterization of Xanthan gum-based hydrogel with Fe3+ ions coordination and its reversible sol-gel conversion, *Carbohydr Polym*, 203 (2019) 139.

2 Mohsin A, Zaman W Q, Guo M, Ahmed W, Khan I M, Niazi S, Rehman A, Hang H & Zhuang Y, Xanthan-curdlan nexus for synthesizing edible food packaging films, *Int J Biol Macromol*, 162 (2020) 43.

3 Farris S, Schaich K M, Liu L S, Piergiovanni L & Yam K L, Development of polyion-complex hydrogels as an alternative approach for the production of bio-based polymers for food packaging applications: A review, *Trends Food Sci Technol*, 20 (2009) 316.

4 Garavand F, Rouhi M, Razavi S H, Cacciotti I & Mohammadi R, Improving the integrity of natural biopolymer films used in food packaging by crosslinking approach: A review, *Int J Biol Macromol*, 104 (2017) 687.

5 Batista R A, Espitia P J P, Quintans J S S, Freitas M M, Cerqueira M A, Teixeira J A & Cardoso J C, Hydrogel as an alternative structure for food packaging systems, *Carbohydr Polym*, 205 (2019) 106.

6 Kaur M & Santhiya D, UV-shielding antimicrobial zein films blended with essential oils for active food packaging, *J Appl Polym Sci*, 138 (2021) 1.

7 Bueno V B, Bentini R, Catalani L H & Petri D F S, Synthesis and swelling behavior of xanthan-based hydrogels, *Carbohydr Polym*, 92 (2013) 1091.

8 Malik N S, Ahmad M, Minhas M U, Tulain R, Barkat K, Khalid I & Khalid Q, Chitosan/xanthan gum based hydrogels as potential carrier for an antiviral drug: Fabrication, characterization, and safety evaluation, *Front Chem*, 8 (2020) 50.

9 Zhu J, Guan S, Hu Q, Gao G, Xu K & Wang P, Tough and pH-sensitive hydroxypropyl guar gum/polyacrylamide hybrid double-network hydrogel, *Chem Eng J*, 306 (2016) 953.

10 Parameswaran-Thankam A, Al-Anbaky Q, Al-karakooly Z, Rangu-Magar A B, Chhetri B P, Ali N & Ghosh A, Fabrication and characterization of hydroxypropyl guar-poly (vinyl alcohol)-nano hydroxyapatite composite hydrogels for bone tissue engineering, *J Biomater Sci Polym Edn*, 29 (2018) 2083.

11 Simões B M, Cagnin C, Yamashita F, Olivato J B, Garcia P S, de Oliveira S M & Grossmann M V E, Citric acid as crosslinking agent in starch/xanthan gum hydrogels produced by extrusion and thermopressing, *LWT-Food Sci Technol*, 125 (2020) 108950.

12 Ma Q, Ren Y & Wang L, Investigation of antioxidant activity and release kinetics of curcumin from tara gum/ polyvinyl alcohol active film, *Food Hydrocoll*, 70 (2017) 286.

13 Sun C, Xu C, Mao L, Wang D, Yang J & Gao Y, Preparation, characterization and stability of curcumin-loaded zein-shellac composite colloidal particles, *Food Chem*, 228 (2017) 656.

14 Wang H, Gong X, Guo X, Liu C, Fan Y Y, Zhang J, Niu B & Li W, Characterization, release, and antioxidant activity of curcumin-loaded sodium alginate/ZnO hydrogel beads, *Int J Biol Macromol*, 121 (2019) 1118.

15 Kianpour S, Ebrahiminezhad A, Mohkam M, Tamaddon A M, Dehshahri A, Heidari R & Ghasemi Y, Physicochemical and biological characteristics of the nanostructured polysaccharide-iron hydrogel produced by microorganism Klebsiella oxytoca, *J Basic Microbiol*, 57 (2017) 132.

16 Zhang Q, Hu X M, Wu M Y, Wang M M, Zhao Y Y & Li T T, Synthesis and performance characterization of poly(vinyl alcohol)-xanthan gum composite hydrogel, *React Funct Polym*, 136 (2019) 34.

17 Lu X, Li Y, Feng W, Guan S & Guo P, Self-healing hydroxypropyl guar gum/poly (acrylamide-co-3-acrylamidophenyl boronic acid) composite hydrogels with yield phenomenon based on dynamic PBA ester bonds and H-bond, *Colloids Surfaces A Physicochem Eng Asp*, 561 (2019) 325.

18 Nawaz A, Farid A, Safdar M, Latif M S, Ghazanfar S, Akhtar N, Al-Jaouni S K, Selim S & Khan M W, Formulation development and Ex-vivo permeability of curcumin hydrogels under the influence of natural chemical enhancers, *Gels*, 8 (2022) 1.

19 Tanwar R, Kumar L, Kumar P & Gaikwad K K, Characterization of guar gum based edible film containing microwave-assisted mint leaves extract and citric acid for ber (Ziziphus Mauritiana) fruit packaging, *SSRN Electron J*, (2021) 3978979.

20 Yanhan Q, Shucai L, Zhaofeng L, Jian Z & Haiyan L, Hydration effect of sodium silicate on cement slurry doped with xanthan, *Constr Build Mater*, 223 (2019) 976.

21 Katherine R F, Muthukumaran C, Sharmila G, Kumar N M, Tamilarasan K & Jaiganesh R, Xanthan gum production using jackfruit-seed-powder-based medium: Optimization and characterization, *3 Biotechnol*, 7 (2017) 248.

22 Chen X, Li P, Kang Y, Zeng X, Xie Y, Zhang Y, Wang Y & Xie T, Preparation of temperature-sensitive Xanthan/NIPA hydrogel using citric acid as crosslinking agent for bisphenol A adsorption, *Carbohydr Polym*, 206 (2019) 94.

23 Horn M M, Martins V C A & de Guzzi P A M, Influence of collagen addition on the thermal and morphological properties of chitosan/xanthan hydrogels, *Int J Biol Macromol*, 80 (2015) 225.

24 Williams P D, Oztop M H, Mccarthy M J, Mccarthy K L & Lo Y M, Characterization of water distribution in xanthan-curdlan hydrogel complex using magnetic resonance imaging, nuclear magnetic resonance relaxometry, rheology, and scanning electron microscopy, *J Food Sci*, 76 (2011) 472.

25 Singh B & Singh B, Graft copolymerization of polyvinylpyrollidone onto Azadirachta indica gum polysaccharide in the presence of crosslinker to develop hydrogels for drug delivery applications, *Int J Biol Macromol*, 159 (2020) 264.

26 Singh B, Sharma S & Dhiman A, Acacia gum polysaccharide based hydrogel wound dressings: Synthesis, characterization, drug delivery and biomedical properties, *Carbohydr Polym*, 165 (2017) 294.

27 Manna P J, Mitra T, Pramanik N, Kavitha V, Gnanamani A & Kundu P P, Potential use of curcumin loaded carboxymethylated guar gum grafted gelatin film for biomedical applications, *Int J Biol Macromol*, 75 (2015) 437.

28 Singh B & Sharma N, Mechanistic implication for cross-linking in sterculia-based hydrogels and their use in GIT drug delivery, *Biomacromolecules*, 10 (2009) 2515.

29 Liepsch D, A basic introduction to rheology shear flow, *J Biomech*, 35 (2016) 415.

30 Wang C S, Virgilio N, Carreau P J & Heuzey M C, Understanding the effect of conformational rigidity on rheological behavior and formation of polysaccharide-based hybrid hydrogels, *Biomacromolecules*, 22 (2021) 4016.

31 Merlusca I P, Ibanescu C, Tuchilus C, Danu M, Atanase L I & Popa I M, Characterization of neomycin-loaded xanthan-chitosan hydrogels for topical applications, *Cellul Chem Technol*, 53 (2019) 709.

32 Yadav R & Purwar R, Influence of metal oxide nanoparticles on morphological, structural, rheological and conductive properties of mulberry silk fibroin nanocomposite solutions, *Polym Test*, 93 (2021) 106916.

33 Herrada-Manchón H, Rodríguez-González D, Fernández M A, Kucko N W, De G F B & Aguilar E, Effect on rheological properties and 3D printability of biphasic calcium phosphate microporous particles in hydrocolloid-based hydrogels, *Gels*, 8 (2022) 28.

34 Stojkov G, Niyazov Z, Picchioni F & Bose R K, Relationship between structure and rheology of hydrogels for various applications, *Gels*, 7 (2021) 255.

35 Ajovalasit A, Sabatino M A, Todaro S, Alessi S, Giacomazza D, Picone P, Carlo M D & Dispenza C, Xyloglucan-based hydrogel films for wound dressing: Structure-property relationships, *Carbohydr Polym*, 179 (2018) 262.

36 Raschip I E, Fifere N, Varganici C D & Dinu M V, Development of antioxidant and antimicrobial xanthan-based cryogels with tuned porous morphology and controlled swelling features, *Int J Biol Macromol*, 156 (2020) 608.

37 Rukmanikrishnan B, Ismail F R M, Manoharan R K, Kim S S & Lee J, Blends of gellan gum/xanthan gum/zinc oxide based nanocomposites for packaging application: Rheological and antimicrobial properties, *Int J Biol Macromol*, 148 (2020) 1182.

38 Valdés A, Ramos M, Beltrán A, Jiménez A & Garrigós M C, State of the art of antimicrobial edible coatings for food packaging applications, *Coatings*, 7 (2017) 1.

39 Liu Y, Wang S, Lan W & Qin W, Fabrication and testing of PVA/Chitosan bilayer films for strawberry packaging, *Coatings*, 7 (2017) 1.

40 Wang L F & Rhim J W, Preparation and application of agar/alginate/collagen ternary blend functional food packaging films, *Int J Biol Macromol*, 80 (2015) 460.

41 Bhoopathy S, Inbakandan D, Rajendran T, Chandrasekaran K, Kasilingam R & Gopal D, Curcumin loaded chitosan nanoparticles fortify shrimp feed pellets with enhanced antioxidant activity, *Mater Sci Eng C*, 120 (2021) 111737.

42 Suresh D, Shobharani R M, Nethravathi P C, Kumar P M A, Nagabhushana H & Sharma S C, Artocarpus gomezianus aided green synthesis of ZnO nanoparticles: Luminescence, photocatalytic and antioxidant properties, *Spectrochim Acta-Part A Mol Biomol Spectrosc*, 141 (2015) 128.

43 Singh B & Rajneesh, Gamma radiation synthesis and characterization of gentamicin loaded polysaccharide gum based hydrogel wound dressings, *J Drug Deliv Sci Technol*, 47 (2018) 200.

44 Nissa R C, Fikriyyah A K, Abdullah A H D & Pudjiraharti S, Preliminary study of biodegradability of starch-based bioplastics using ASTM G21-70, dip-hanging, and soil burial test methods, *IOP Conf Ser Earth Environ Sci*, 277 (2019) 012007.